Chế tạo vật liệu siêu hấp thụ dựa trên dẫn xuất chitosan ứng dụng trong nông nghiệp

TÓM TẮT

Nghiên cứu đã tận dụng thành công vỏ tôm để chiết tách chitosan bằng quy trình deacetyl hóa hai bước với độ deacetyl hóa cao (91,48%). Hơn nữa, nghiên cứu đã khắc phục thành công tính tan kém của chitosan trong môi trường pH trung tính và kiềm bằng cách gắn các nhóm chức vào chuỗi chính của chitosan, tăng độ tan của chitosan trong môi trường pH > 6,5. Tiếp theo là ghép dẫn xuất chitosan với axit acrylic (AA) để tạo ra vật liệu polyme siêu hấp thụ từ O-carboxymethyl chitosan (OCMCS-SAP) với khả năng hấp phụ tối đa là 658,16 g/g sau 15 ngày ngâm trong nước. Đồng thời, các thông số tối ưu để tổng hợp vật liệu là nồng độ kali persufate 2%, tỷ lệ O-CMCS:AA là 1:8 và nồng độ glutaraldehyde 2%. Khả năng phân hủy sinh học sau bốn tuần thử nghiệm và giữ nước để cung cấp cho cây trong quá trình sinh trưởng là điểm mạnh của vật liệu OCMCS-SAP. Ngoài ra, nghiên cứu đã thành công trong việc phân tích sự hình thành và sinh trưởng của hai cây ớt giống nhau, nhưng khác nhau ở việc có và không có sử dụng OCMCS-SAP. Cây ớt sử dụng OCMCS-SAP có khả năng sinh trưởng và phát triển cao hơn nhiều so với cây không sử dụng OCMCS-SAP. Sau tám tuần thử nghiệm, những cây không được tưới nước cho thấy lá héo và phát triển cực kỳ thấp. Dựa trên tất cả các phát hiện thực nghiệm, vật liệu OCMCS-SAP đã được tổng hợp thành công và có tiềm năng được ứng dụng để cải tạo đất khô cằn.

Từ khoá: *Vật liệu siêu hấp thụ, dẫn xuất chitosan, trương nở, giữ nước*

Fabrications of chitosan-derivative-based superabsorbent materials for agriculture application

ABSTRACT

The study successfully utilized shrimp shells to extract chitosan using a two-step deacetylation process with a high degree of deacetylation (91.48%). By adding functional groups to the chitosan's main chain, the study was also able to overcome the chitosan's poor solubility in neutral and alkaline pH environments, making it more soluble in pH environments higher than 6.5. Following a 15-day immersion in water, the chitosan derivative was grafted with acrylic acid (AA) to produce a superabsorbent polymer material from O-carboxymethyl chitosan (OCMCS-SAP) with a maximum adsorption capacity of 658.16 g/g. The ideal conditions for the material's synthesis were a 2% glutaraldehyde concentration, a 1:8 O-CMCS:AA ratio, and a 2% potassium persulfate concentration. The OCMCS-SAP material's strengths are its capacity to hold onto water to support the plants throughout growth and its biodegradability following four weeks of testing. Furthermore, the study effectively examined how two identical chili plants developed and changed in the presence and absence of OCMCS-SAP. Compared to plants lacking OCMCS-SAP, the chili plants with OCMCS-SAP grew and developed significantly more. Following eight weeks of testing, the water-deficient plants had wilting leaves and remarkably slow development. The OCMCS-SAP material was effectively synthesized and may be used to enhance arid soil, according to all experimental results.

Keywords: *Superabsorbent materials, chitosan derivatives, swelling, water retention*

1. INTRODUCTION

Superabsorbent polymers (SAP) are currently the subject of extensive research in Vietnam and are gradually being commercialized. However, modified starch - which may compete with human and animal food sources - is the primary basic material used by the majority of authors. Khoi et al. (2003) successfully created the first superabsorbent polymer for soil (AMS-1). The product known as AMS-1 is made by grafting acrylic acid into cassava starch, which has a unique capacity to store and absorb water. AMS-1 is a fine, ivory-white powder that will swell 400 times its actual weight when exposed to water. It can be stored in soil for 10 to 12 months. AMS-1 has a wide range of uses in agricultural production, including helping to improve the physical and chemical properties of soil and acting as a moisture-retaining agent on hillsides where water readily drains away or on dry, sandy soils. Apart from its ability to absorb water, AMS-1 can also absorb other solutions, such as saline and urine.[1]

Furthermore, Lac Trung Company produced the superior product known as superabsorbent polymer (SAM-1) in 2006. The product is the end product of the polymerization of modified cassava starch and acrylic acid. Each tiny moisture-retaining particle can absorb up to 350–400 g/g of water and then gradually release it to provide moisture for the plant during times when there is no rain or irrigation water. The primary ingredient is cassava starch, and chemical technology is used to create a type of polymer that has the ability to absorb and retain water. Watering will be much decreased after 30 to 45 days when the particles will release all of the water, the moisture-retaining particles will revert to their initial size, and they will continue to collect water when it rains or is watered. Moisture-retaining particles should be used for six to eighteen months before being replaced. Utilizing the product has been shown to reduce plant mortality by over 100%, lower plant care expenses by up to 80%, transport crops across great distances, and harvest crops 20% earlier than planned.[2]

Khan et al. synthesized superabsorbent polymers in 2015 by combining gamma radiation with carboxymethylated cellulose (CMC) and acrylic

acid (AA). In particular, the author synthesized by copolymerizing carboxymethylated cellulose and acrylic acid and then irradiating it with Co-60. Due to the extremely high energy of the gamma irradiation source, initiators, catalysts, and cross-linking agents are not required in the synthesis technique. At the same time, a radiation dose of 5 kGy was shown to have the maximum adsorption capability. According to experimental results, the product's high water retention capacity had a favorable impact on the germination of okra and wheat seeds as well as the growth of young plants. Thus, it can be said that CMC/AA, which has a lot of great qualities, can be employed as a regulator in agriculture, particularly in desert and arid areas.[3]

A superabsorbent water gel (CHCAUR) was created by Narayanan et al. (2018) using urea, citric acid, and chitosan. A superabsorbent material was developed from renewable resources such as chitosan, citric acid and urea by hydrothermal method. The maximum adsorption was about 1250 g/g in distilled water and 210 g/g in 0.1% sodium chloride solution. It is demonstrated that the water absorption mechanism results from the electrostatic attraction of water for ionic bonding, the presence of pores, and the undulating surface caused by the development of nanofibers. It was demonstrated that physical bonds, such as electrochemical bonds, macropores, and morphological characteristics, are the source of the water absorption. It was found that CHCAUR had a very high chitosan content and a low urea/citric acid content, making it highly biodegradable in soil. With a significant and regulated water output, the product was employed to supply nutrients to the soil. CHCAUR was also shown to dramatically lower the rate of water evaporation when applied to soil.[4]

In 2018, Neamjan et al. reported on the biodegradable superabsorbent polymer based on cellulose from sugarcane bagasse (SCB) for water resource management, horticulture and other products in agricultural applications. Specifically, the superabsorbent polymer was prepared by polymerizing SCB monomer and AA in the presence of N, N-methylene-bisacrylamide as a cross-linker using twin screw extruder and using ammonium persulfate/sodium sulfite (APS/SS) as a pair initiator in an enhanced redox system because SS is a reducing agent that can enhance the polymerization reaction. The results indicated that the soil moisture retention capacity could be enhanced by applying SCB superabsorbent polymer. Therefore, the superabsorbent polymers prepared in this study have the potential to be used as a water source in agriculture.[5]

According to Yassine et al. (2024), the extracted cellulose in superabsorbent materials with high water absorption capabilities was oxidized by sodium periodate in a controlled manner to produce cellulose dialdehyde with a regulated aldehyde content. Using N,N-methylene-bis-acrylamide as a cross-linking agent and potassium persulfate as an initiator, the cellulosic materials were mixed with a suspension of acrylic and itaconic acids to create composite hybrid hydrogels through radical chain polymerization in water. Notably, dialdehyde cellulose has the potential to improve the hydrogel's swelling and water retention ability because of its strong polarity, low crystallinity index, and hydrophilicity. With a dialdehyde cellulose content of 5%wt, synthesized materials demonstrated a water absorption capacity of up to 1240±60 $g.g^{-1}$.[6]

One of the most important issues of concern today in the agricultural sector is watering plants during the drought season while still ensuring that enough water is provided for the plants during their growth and development, avoiding waterlogging due to over-watering or reducing the mortality rate of plants during the dry season, etc. To help solve this problem, a new material has been researched and widely applied by many researchers in many places around the world, which is superabsorbent polymer (SAP). This material is widely used in agriculture, sanitary napkins, medicine, and other fields because it can absorb and retain a lot of water in its structure - many times more than its dry weight. In the agricultural sector, SAP application can lower plant mortality rates from dehydration, reduce care, watering frequency, water amount, pesticide residues, pre-season harvesting, etc. Nonetheless, modified starch and acrylic acid provide the majority of the produced SAP.[7,8] However, the use of starch to synthesize SAP results in a very serious waste of food sources, a source of nutrition for both humans and animals, as well as intense competition between humans and animals for food sources. This is because starch is still an important food source, both for humans and animals. Therefore, in this study, we extract chitosan for SAP manufacture utilizing "shrimp shells," a waste product that is typically discarded and has a significant risk of creating environmental damage, rather than starch. The primary drawback of CS is its poor solubility in neutral and alkaline pH environments. For this

reason, in this study, we modify CS and produce CS derivatives (by adding hydrophilic groups to the CS structure to make CS more soluble in an environment with a pH greater than 6.5) in order to synthesize SAP. Since SAP materials are made from natural raw materials, such as seafood waste, they are highly biodegradable, environmentally benign, and satisfy the "green chemistry" standards that our nation is striving for in the future while creating new materials. Research on the synthesis of biodegradable superabsorbent polymer (SAP) from chitosan derivatives and its application in agriculture based on the following steps: synthesis of SAP material, analysis of adsorption-influencing factors, analysis of adsorption and desorption capacity, and analysis of the product's biodegradability over time in a soil environment.

2. MATERIALS AND METHODS

2.1 Materials

Fresh shrimp shells are gathered from the Chau Thanh District of Kien Giang Province's Bright Star Seafood Company Limited. Following gathering, the shrimp shells undergo numerous water washes to clean them before being dried and used.

Sodium hydroxide (NaOH, 99%), oxalic acid ($C_2H_2O_4$, 99.6%), hydrochloric acid (HCl), potassium persulfate ($K_2S_2O_8$), acetic acid (CH_3COOH, 99.5%), chloroacetic acid ($ClCH_2COOH$), acrylic acid (CH_2=$CHCOOH$, 99.5%), and glutaraldehyde ($C_5H_8O_2$, 50%) were acquired from Xilong, China. All other chemicals were of reagent grades or higher and used as received.

2.2 Preparation of chitosan derivatives from shrimp shells by chemical method

The chemical process of creating chitosan derivatives from shrimp shells was carried out in two stages. Chitosan was first extracted from shrimp shells using a chemical process that involved two rounds of deacetylation. This was followed by the production of chitosan derivatives using O-carboxymethyl. The synthesis of chitosan from shrimp shells was based on the optimal parameters of the synthesis process of Kurniasih et al. (2014) and several steps were modified to fit Vietnamese research settings.[9] The synthesis diagram is presented specifically in Figure 1.

Figure 1. Chitosan preparation using shrimp shells

The shrimp shells were initially collected at Ngoi Sao Tuoi Sang Seafood Company, the shrimp shells were refrigerated with ice while being transported. After processing, the shrimp shells were cleaned to get rid of any remaining shrimp meat, debris, and contaminants. To preserve the shrimp shells for the upcoming tests, they were then dried. Following first treatment, the shrimp shells were soaked in a 2M NaOH solution for two days in order to separate the protein and fat. At this point, alkali at pH 11–12 and room temperature degraded the protein to produce soluble free amines that were simple to remove after the shrimp shells were cleaned with water. Following multiple water washes, the product was ultimately cleaned with distilled water until its pH reached 7. The shrimp shells were then demineralized using a 1M HCl solution for 48 hours at room temperature in order to extract calcium and a few other minerals. Crude chitin was treated with 1% oxalic acid and 1%

$KMnO_4$ oxidant for 15 minutes at room temperature in order to eliminate the pale pink astaxanthin color. Lastly, a 48% NaOH solution was used to deacetylate crude chitin (-$NHCOCH_3$) to chitosan (-NH_2) for 48 hours at room temperature. To produce chitosan with a larger degree of deacetylation, same procedure was carried out again, but at a higher temperature (80°C). Chitosan was dried for 12 hours at 50°C in order to preserve it.

The method of Mohamed et al. (2017) provides the basis for the synthesis of O-carboxymethyl chitosan (O-CMCS), which has high solubility in neutral and alkaline pH by attaching hydroxyl groups to the chitosan structure. However, certain variables have been modified to suit Vietnam. Figure 2 specifically displays the O-CMCS synthesis diagram. First, in a three-necked flask, 100 mL of 20% NaOH solution was mixed with 10 g of second deacetylated chitosan (CS-DD2) and stirred for 15 minutes. The carboxymethylation process was then carried out by adding 15 g of monochloroacetic acid and 20 mL of 2-propanol dropwise to the alkalized liquid and keeping the reaction at 40°C for two hours. 10% acetic acid was used to neutralize the liquid after two hours, bringing its pH down to 7. After removing insoluble substances with 70% EtOH, the product was washed with absolute EtOH. Finally, the O-CMCS product was then dried at 50°C.

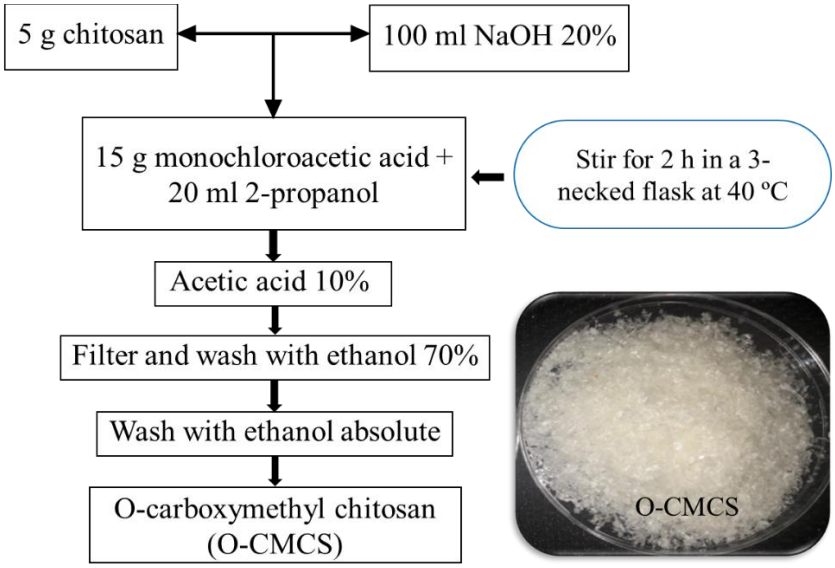

Figure 2. Synthesis diagram of O-CMCS synthesis from chitosan

2.3 Synthesis of superabsorbent polymers (SAP) from chitosan derivatives

Superabsorbent polymer (SAP) was synthesized from chitosan derivative (O-CMCS) in a 250 mL glass beaker that was submerged in silicone oil and had a magnetic stirrer that was heated to 60-70 °C throughout the reaction. The experiment was carried out by dispersing 1 g of O-carboxymethyl chitosan (O-CMCS), which was synthesized in the previous step, evenly in distilled water. Next, the initiator ($K_2S_2O_8$), monomer ($CH_2CHCOOH$), and cross-linker (glutaraldehyde) were added one after the other while being continuously stirred on a heated magnetic stirrer for a predetermined amount of time. The reaction mixture from the previous step was then allowed to cool to room temperature and neutralized with 3% NaOH to reach pH 7. Methanol was then added while stirring. Following the completion of the reaction, the product is crushed and dried for 48 hours at 50°C. At this point, OCMCS-SAP material is obtained. In particular, Figure 3 displays the material synthesis diagram.

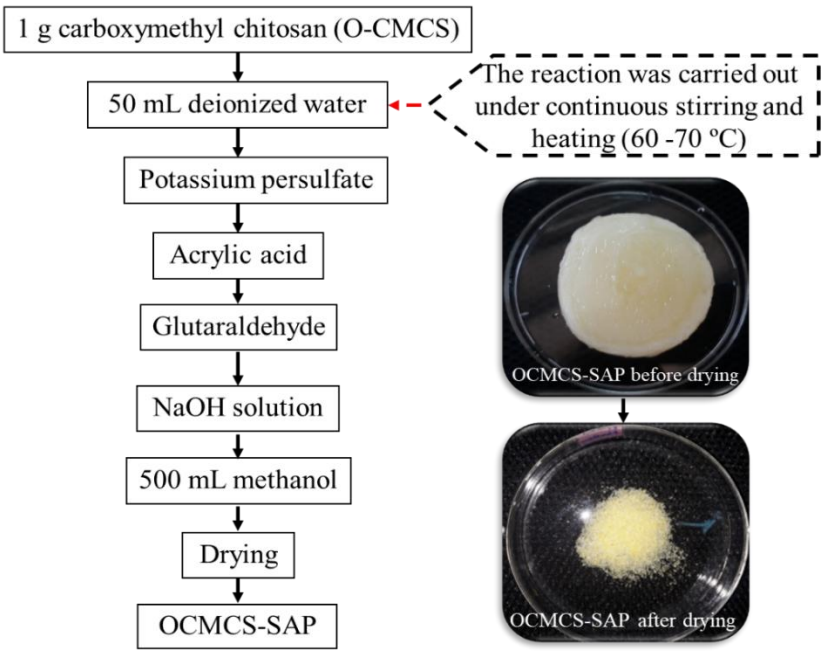

Figure 3. Synthesis diagram of OCMCS-SAP

2.4 Characterizations

The surface images of the samples, including first deacetylated chitosan, second deacetylated chitosan, O-carboxymethyl chitosan, and superabsorbent materials from O-carboxymethyl chitosan, were observed using an optical microscope (Nikon EPIPHOT 200, Japan) and a scanning electron microscope (SEM, S-4800, Hitachi, Japan). The chemical structure of the investigated samples was investigated using Fourier-transform infrared spectroscopy (FTIR, Nicolet 6700, Thermo Scientific, USA). The scanning was performed 32 times under the condition of the wave number of 4000-400 cm^{-1} and the resolution of 4 cm^{-1}. The crystallographic structure was determined using X-ray diffraction (XRD, Empyrean, PANalytical). The material's thermal stability was assessed using thermogravimetric analysis (TGA, Q500 V20.10), which determined the material's temperature range of 50 to 600°C in an inert nitrogen environment at a rate of 5°C per minute.

3. RESULTS AND DISCUSSION

The chitosan samples that were deacetylated once (CS-DD1) and twice (CS-DD2) had clear color variations, as seen in Figures 4a and 4b. The CS-DD2 product was bright white, whereas the CS-DD1 product was ivory yellow. Both products shared the trait of being odorless. Additionally, through the acid-base titration method, the deacetylation degree of CS-DD1 sample was 79.68% and the deacetylation degree of CS-DD2 sample was 91.48%, which were much higher than those of CS-DD1 sample.

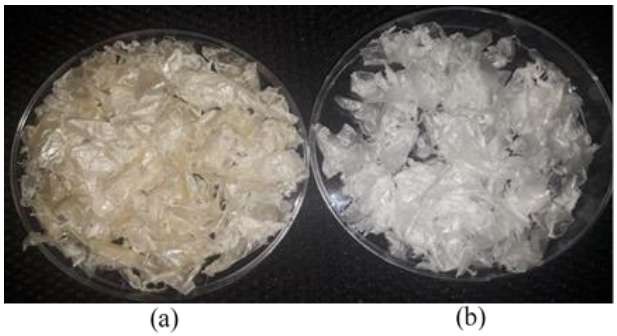

Figure 4. CS-DD1 (a) and CS-DD2 (b)

3.1 Investigation results of factors affecting the adsorption capacity of OCMCS-SAP

3.3.1. Effect of potassium persulfate (KPS) concentration

By adjusting the KPS concentration from 1 to 2.5% while maintaining the same reaction temperature (60-70°C), O-CMCS:AA ratio (1:6), and glutaradehyde concentration of 1.5%, the impact of KPS concentration on water adsorption was examined. In Figure 5, the water adsorption outcomes of four samples with varying KPS concentrations are explicitly displayed.

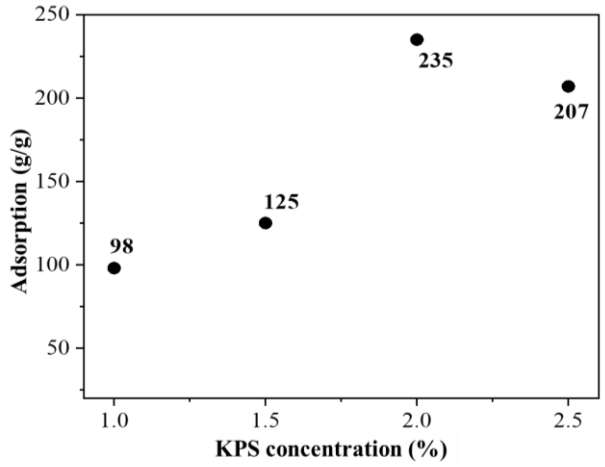

Figure 5. Results of the influence of KPS concentration on water adsorption of OCMCS-SAP

The impact of the initiator (KPS) on the polymer's swelling was depicted in Figure 5. As the KPS concentration rose from 1 to 2.5%, the swelling ratio of the polymer in distilled water changed. This was because the higher KPS concentration led to a greater number of free radicals, which in turn produced more macro-radicals in the main chain of OCMCS-SAP, and the shorter kinetic chain length resulted in poor water adsorption. Meanwhile, as Figure 5 illustrates, a KPS concentration of 2% was appropriate for the development of extremely inflated products. The material's adsorption capacity in distilled water, however, decreased as the KPS concentration was raised further because more free radicals would improve the reaction termination step through molecular collisions and the molecular weight of the branch chains would decrease.

3.3.2 The effect of acrylic acid (AA) concentration

The results of the water adsorption of four samples are shown in Figure 6 specifically. The effect of AA concentration on water adsorption was investigated by changing the O-CMCS:AA ratio from 1:2 to 1:10 while maintaining the parameters such as reaction temperature 60-70°C, KPS concentration of 2%, and glutaradehyde concentration of 1.5%. Since AA is the primary water adsorption group, more AA molecules will be grafted into the OCMCS structure as the AA ratio rises. This will boost the material's water adsorption and make OCMCS-SAP more hydrophilic. However, increasing the OCMCS-SAP:AA ratio to 1:10 only increases the material's water adsorption by 5% (insignificant), hence the OCMCS-SAP ratio of 1:8 is the best option for creating a material with high water adsorption while remaining economical. On the other hand, increasing the AA concentration too high reduces the material's swelling ratio because increasing the AA concentration raises the viscosity of the product and inhibits the mobility of free radicals, lowering the ability to absorb water.

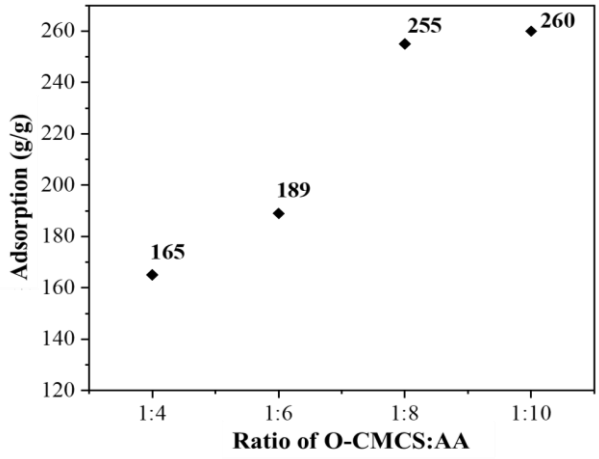

Figure 6. Results on the effect of AA concentration on water adsorption

3.3.3 Effects of glutaraldehyde concentration

The effect of glutaradehyde concentration on water adsorption was investigated by increasing the glutaradehyde concentration from 1 to 3% while maintaining the parameters such as reaction temperature 60-70°C, KPS concentration 2%, and O-CMCS:AA ratio 1:8. The water adsorption results of 5 samples are shown specifically in Figure 7. When the amount of cross-linking agent (glutaradehyde) is insufficient, the swelling ratio of OCMCS-SAP is low, as the low cross-linking density cannot sustain the adsorbed water when measuring the swelling ratio by filtration. Simultaneously, the material's capacity to adsorb water steadily increases as the amount of glutaradehyde grows, and the swelling ratio achieves its maximum value when the glutaradehyde concentration approaches 2%. Because excessive cross-linking produces a dense network structure that results in poor water adsorption, the material's absorption capacity falls as cross-linking increases. This indicates that 2% glutaradehyde is appropriate for producing a product with a high water absorption rate.

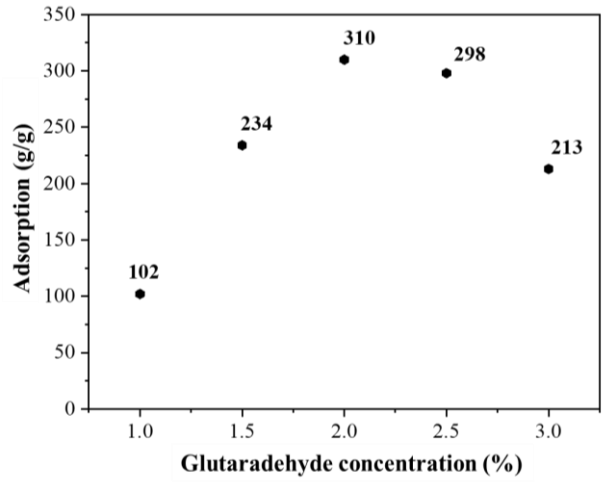

Figure 7. Results on the effect of glutaradehyde concentration on water adsorption

3.2 Investigation of adsorption and desorption capacity of OCMCS-SAP materials

The investigation into the water absorption of OCMCS-SAP material lasted for 30 days, and the findings of the material's water absorption ability are shown in particular in Figure 8.

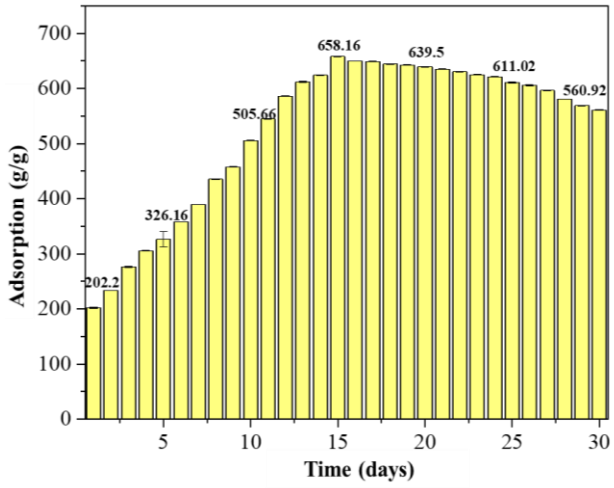

Figure 8. Results on water absorption capacity of OCMCS-SAP material in 30 days

After five days, the material's water absorption capacity grew steadily from 202.2 g/g to 326.16 g/g, and after ten days, it reached 505.66 g/g. Nevertheless, the material's capacity to absorb water rose further, reaching a very high 658.16 g/g when the duration was extended to 15 days. This is because, as survey time increases, so do the hydrogen bonding and Van der Waals (collision) forces between water molecules and the super adsorbent. The water absorption trend, however, declined dramatically after 15 days, as evidenced by the material's water absorption capacity dropping to 639.5 g/g on day 20, continuing to decline accordingly on day 25, and reaching only roughly 560.92 g/g on day 30. The primary cause of inadequate water absorption is the material's degradation during 15 days of swelling, which is regarded as the adsorption release period if it lasts for 15 days or longer and occurs after the material has attained the ideal adsorption condition.

Following the examination of the material's water adsorption capacity, a 30-day test of the material's water desorption capability was also conducted, as shown in Figure 9. In particular, the material only discharged only 2.4% of its water content in the first five days, but over time, this percentage grew steadily. The material's adsorption release trend significantly increased starting on day 15. The material usually released approximately 85.5% on day 16, and then started to leak substantially (~78%) on day 17. This is because evaporation on the material's surface over time and osmotic pressure differ. The material saw a strong adsorption release phase from day 25 to day 30, and as the graph illustrates, after 30 days, the material achieved an adsorption release of roughly 49.5% (relatively lower than the initial weight).

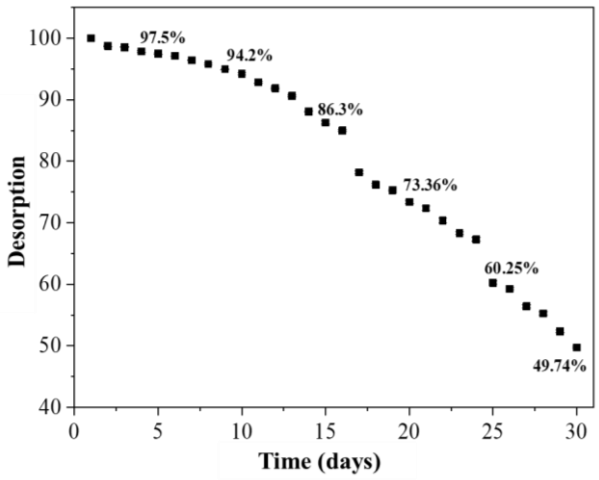

Figure 9. Material desorption test graph after 30 days

3.3 Physicochemical characteristics

The characteristics of the shape and surface structure of CS-DD1, CS-DD2, O-CMCS, and OCMCS-SAP samples were observed with an optical microscope at 50x magnification, shown in Figure 10. Because the fibers contracted, the surface morphology of CS-DD1 showed numerous pores in Figure 10a; however, because these pores were rather narrow, the material was unable to

achieve its super water adsorption objective. Following the second DD with 48% NaOH (80 °C), the CS-DD2 sample's surface morphology is shown in Figure 10b. The initial fibers started to straighten and were easily visible when the surface of the CS-DD2 sample displayed an image of long, straight fibers. The surface morphology of the CS derivative (O-CMCS) is vividly displayed in Figure 10c. In comparison to the CS-DD2 sample, the OCMCS surface no longer contains dense fibers like CS-DD2, but instead has sparser fibers. Additionally, the network connection has expanded, making it easier for water to enter the structure. Because the original structure of CS was destroyed when it was modified with monochloroacetic acid (MA), the network structure expanded when the fibers became sparser. These expanded network holes are crucial for the adsorption of water into the polymer structure, demonstrating that OCMCS is a potential source of raw materials for the synthesis of SAP.

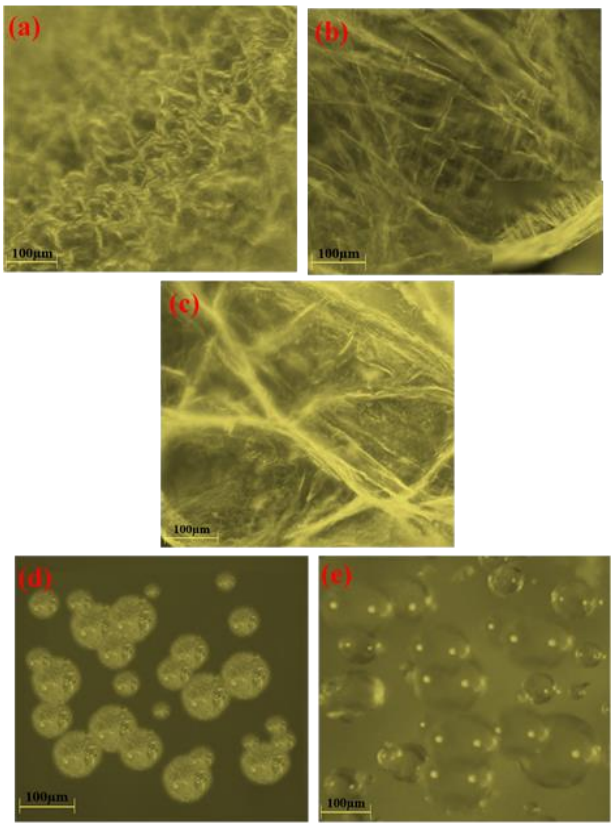

Figure 10. Optical microscope images of CS-DD1 (a), CS-DD2 (b), O-CMCS (c), OCMCS-SAP (d), and OCMCS-SAP after 3 days of swelling (e)

The OCMCS-SAP material's morphology before and after swelling is depicted in Figures 10d and 10e. Despite their spherical form and relatively modest size (d_1 = 96 ± 0.06 μm), the resulting OCMCS-SAP particles exhibit polydispersity, as seen in Figure 10d. But after swelling for three days (d_2 = 373 ± 0.03 μm), the OCMCS-SAP particles in Figure 10e had a diameter that is four times greater than the original particles. After reaching the adsorption state (276.5 g/g), the material particles swelled; however, this is not the material's ideal adsorption state, thus the microparticles will keep growing until the material reaches the ideal adsorption state (15 days of swelling). Optical microscope results showed that the network structure expanded with each stage of production, resulting in a more hydrophilic material. The substance usually had a lot of water after three days of swelling, which resulted in the formation of spherical microparticles. These microparticles are in charge of giving the plant water as it grows and develops.

A scanning electron microscope was then used to examine the OCMCS-SAP material's shape and surface structure both before and after swelling (Figure 11). The OCMCS-SAP particles' surface first developed pores, but in certain places, agglomeration was noticed as a result of overheating during the drying process. After three days of swelling, the material's surface (Figure 11b) changed morphologically as the original pores progressively grew larger. The surface morphology of the material seen was more distinct than in the optical microscopy image, and the presence of pores in the product following adsorption showed that the synthesized material particles were successful and that these pores were crucial in absorbing water to supply water for plants.

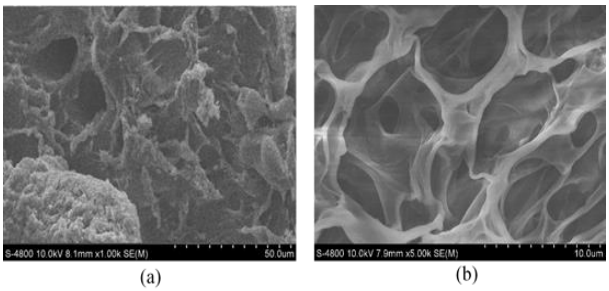

Figure 11. SEM images of (a) OCMCS-SAP and (b) OCMCS-SAP after 3 days of swelling

Figure 12 illustrates the differences in the functional groups of the newly synthesized materials based on the infrared spectra of the CS, O-CMCS, and OCMCS-SAP samples after they were dried.

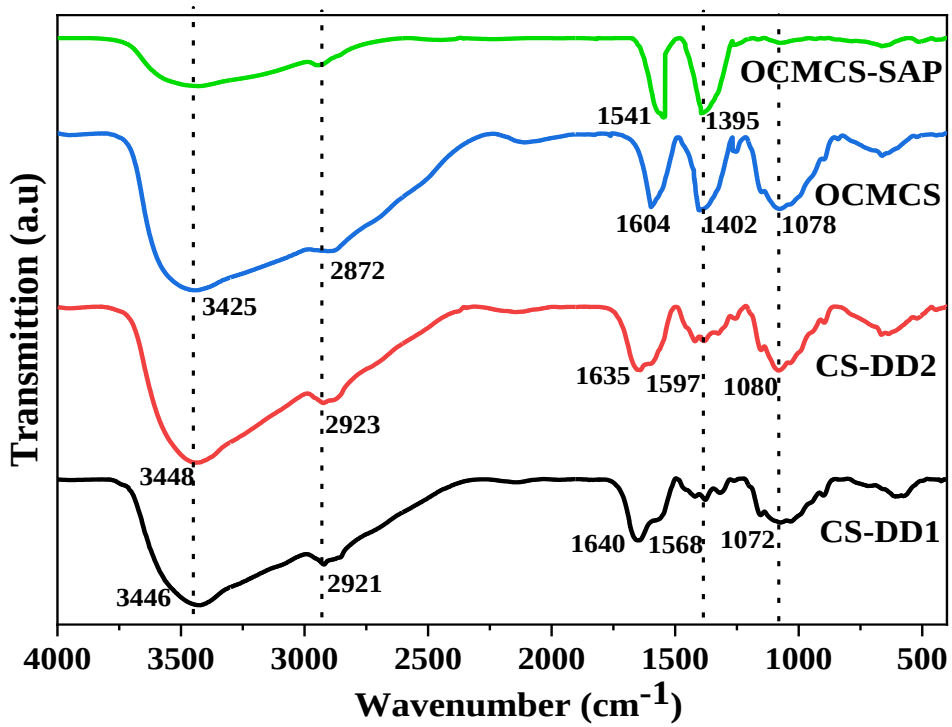

Figure 12. FTIR spectra of CS-DD1, CS-DD2, O-CMCS, and OCMCS-SAP samples

Characteristic vibrations in the FTIR spectrum of CS include O-H and N-H stretching vibrations in the 3350–3450 cm^{-1} range and deformation vibrations of the fatty chain C-H bonds in the 2920–2860 cm^{-1}, 1420 cm^{-1}, and 1380 cm^{-1} ranges, respectively. In-plane N-H bending vibrations are responsible for the formation of high intensity peaks at 1640 cm^{-1} on CS-DD1 and 1635 cm^{-1} on CS-DD2, which is the distinctive peak of polysaccharide on CS. The ether and cyclic glycoside linkages in the CS structure are simultaneously visible in the absorption in the 1000–1300 cm^{-1} range.

The FTIR spectrum of O-CMCS shows the appearance of new peaks with high intensity at wave numbers 1604 cm^{-1} and 1402 cm^{-1}, these bands appear corresponding to the stretching vibration of the C=O bond and the -CH_2COOH vibration, through which we can confirm the appearance of the carboxymethyl group. In addition, the peak 1380 cm^{-1} no longer appears in the spectrum of the CS derivative, which proves that the C-H bond was partially removed when CS reacted with MA.

An additional carboxymethyl chitosan main chain is present in the superabsorbent polymer product's structure, as indicated by the peak in the 1541 cm^{-1} region of the OCMCS-SAP FTIR spectrum. When it appears at the peak of 1395 cm^{-1}, this distinctive band, which is associated with the asymmetric stretching of the carboxylate anion group, is likewise extremely intense. Additionally, there are no odd peaks in the superabsorbent material's FTIR spectra. The OCMCS-SAP product was successfully created when the polymer's AA was grafted onto O-CMCS when glutaraldehyde was present, according to the FTIR data.

X-ray diffraction was used to examine the XRD structures of CS-DD2, CS derivatives, and superadsorbed products (Figure 13). Three primary strong diffraction peaks at 2θ=10.1°, 20.02°, and 22° with high intensity were visible in the XRD analysis results of CS, as illustrated in Figure 8, suggesting that the produced CS had high crystallinity. The production of many hydrogen bonds in the crystal lattice, which resulted in high CS hardness and the development of crystalline areas, was the cause of the high crystallinity of CS. However, following chemical modification, the diffraction peak of the CS derivative (O-CMCS) displayed a decrease in the characteristic peak. This was because the carboxymethyl groups were introduced, increasing the distance between molecular chains and destroying the original structure. Additionally, the number of hydrogen bonds decreased, resulting in an amorphous structure of O-CMCS. The amount of acrylic acid

grafted on the CS derivative structure results in a decrease in crystallinity, which is especially noticeable in the XRD pattern of the superabsorbent product (OCMCS-SAP) when compared to the CS and O-CMCS samples. According to the three materials' XRD data, CS has the highest crystallinity, as seen by the distinctive, highly intense peaks on CS. O-CMCS, which has monochloroacetic acid (MA) grafted onto it, has a lesser crystallinity following chemical transformation. Last but not least, the OCMCS-SAP material sample exhibits the lowest crystallinity, demonstrating the amorphous structure of the composite material and its high water adsorption capacity as a result of its pores. The success of the synthesized material was demonstrated by the XRD analysis of three samples, CS-DD2, O-CMCS, and OCMCS-SAP, as shown in Figure 13. The appearance of distinctive peaks in CS and the decrease in crystallinity following chemical transformation, which results in the material having an amorphous structure, demonstrate the success of the synthesis.

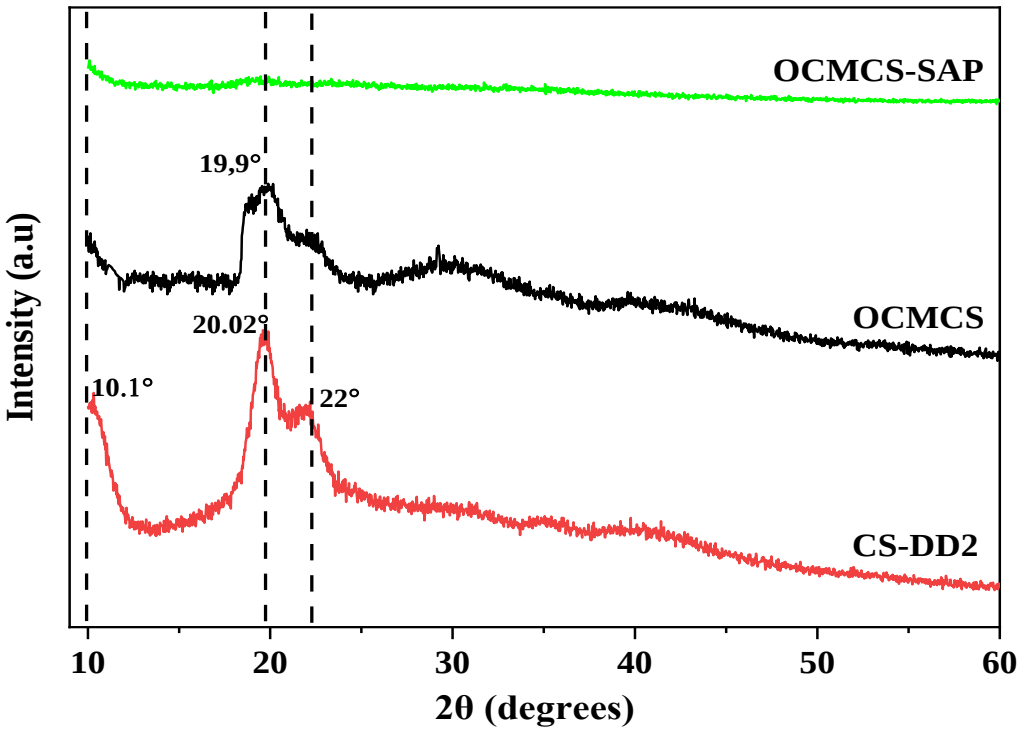

Figure 13. XRD spectra of CS-DD2, O-CMCS, and OCMCS-SAP

Thermogravimetric analysis (TGA) was used to analyze the material samples for thermal stability, and Figure 14 displays the mass loss of the material over various temperature ranges.

A two-stage decomposition mechanism illustrates the thermal breakdown of CS (Figure 14a). Around 100°C is the first stage; the mass loss in this temperature range is associated with the physical adsorption loss of water molecules. At 260–345°C, the second stage of decrease takes place, and at 304°C, the rate of thermal breakdown peaks. The decomposition of the main chain of CS with rising temperature—that is, the oxidation, combustion, and decomposition of deoxidized CS units—could be the cause of this mass loss.

The thermal breakdown for the O-CMCS TGA diagram primarily occurred in three stages, at 170°C, 293°C, and 530°C (Figure 14b). Because the initial thermal decomposition of O-CMCS was at 170°C, the second thermal decomposition interval peaked at 292°C lower than that of CS, and the third thermal decomposition interval reached 530°C, the temperature of the derivative was therefore worse than the decomposition temperature of CS when comparing the TGA diagrams of CS and O-CMCS. It was explained that the original crystal structure of CS was destroyed and the thermal stability of O-CMCS was decreased as a result of the high temperature and alkali breaking the macromolecular chains of CS during the carboxymethylation process.

Figure 14c displays the results of the thermogravimetric study of the O-CMCS-based superabsorbent polymer (OCMCS-SAP). There were four spots of thermal deterioration found. Due to the loss of water in the OCMCS-SAP, the weight loss below 220°C (peaking at 195°C) was the initial step. The breakdown of the polymer's internal groups and branches following graft polymerization resulted in the second stage, which took place between 220°C and 300°C (peaking at 260°C). The third stage was brought on by the breakdown of the carboxymethyl group in the graft copolymer between 300°C and 440°C (peaking at 402°C). The weight loss at this high temperature range suggested that this was the temperature range for polymer chain degradation, as the final reduction stage took place above 440°C (peaking at 483°C). The chitosan-derived grafted superabsorbent (O-CMCS) was shown to have a comparatively high degradation temperature based on the results of thermogravimetric analysis (TGA).

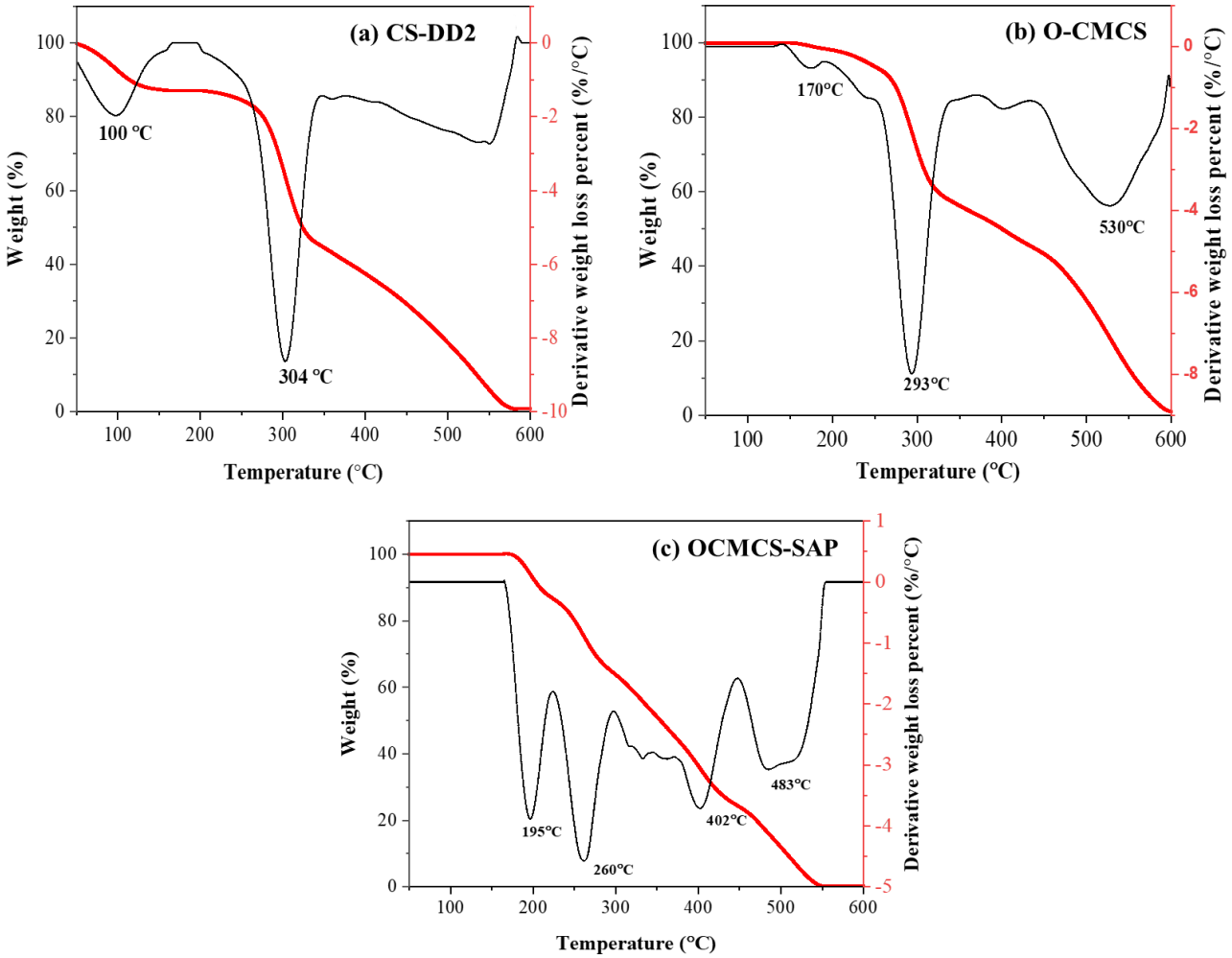

Figure 14. TGA results of CS-DD2, O-CMCS, and OCMCS-SAP

3.4 Examination of OCMCS-SAP's bio-degradability over time in a soil setting

In the soil environment, OCMCS-SAP's bio-degradability over certain time intervals throughout four weeks is shown in Figure 15. As demonstrated throughout the course of the four weeks of the study, the biodegradability of OCMCS-SAP samples generally tends to decrease slightly before and after swelling for dry soil. First, the dry soil decomposes a little in the first week, going down by 0.91% from before swelling, while the sample after swelling shows a phenomena of mass increase, going up by 1.06%. The reason for this is that the material hasn't expanded entirely before burial, thus it's perfectly normal for it to gain bulk after burial. However, after the first week, the material's bulk can be reduced more easily. This is because of the influence of the soil's micro-organisms and the temperature environment. These elements have helped to create the conditions

necessary for the substance to break down in the soil. The biodegradability of the material rose more than it had during the survey weeks. In particular, the pre-swelling sample lost 0.57% of its initial mass, but the post-swelling sample started the biodegradation cycle in the second week and decomposed roughly 0.76% of its starting mass (5 g) by the fourth week. Even though the dry soil survey period was brief, it was sufficient for the material to continue biodegrading in an arid environment while still guaranteeing the ability to supply water to plants under challenging environmental circumstances. This is seen by the material's mass not declining too rapidly over time.

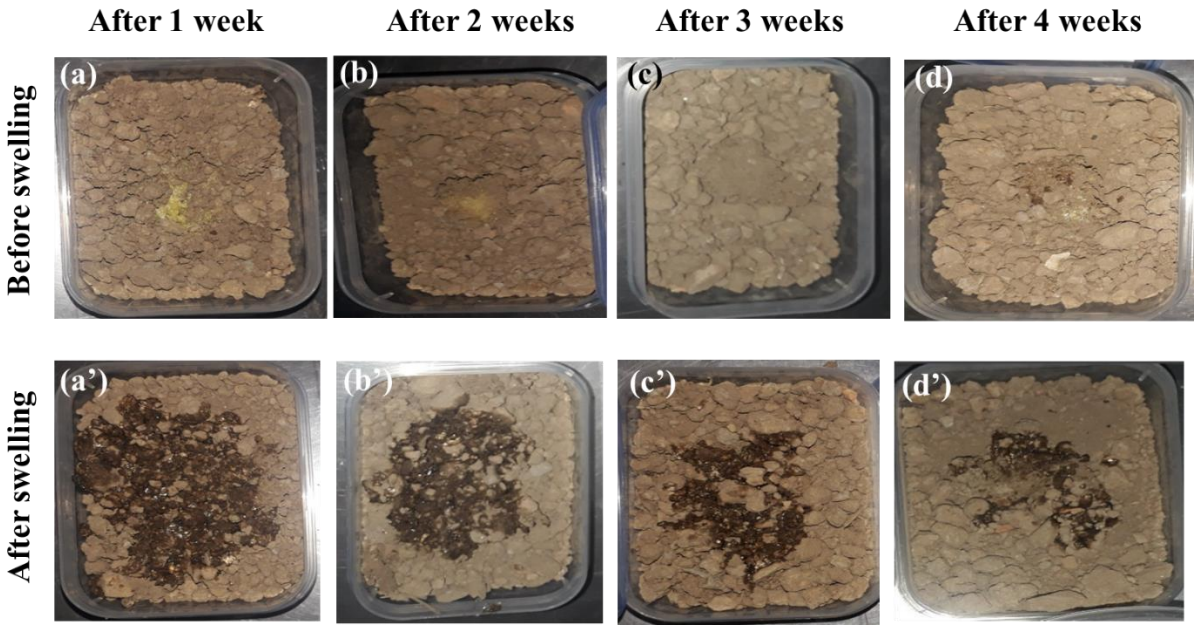

Figure 15. OCMCS-SAP samples in dry soil for biodegradation before and after swelling at different time intervals

Table 1. Experimental results of biodegradability of OCMCS-SAP on dry soil before and after adsorption at different time intervals

	After 1 week	After 2 weeks	After 3 weeks	After 4 weeks
	for OCMCS-SAP sample before adsorption			
Initial mass (g)	0.20	0.20	0.20	0.20
Final mass (g)	0.23	0.21	0.18	0.13
	for OCMCS-SAP sample after adsorption			
Initial mass (g)	5.0	5.0	5.0	5.0
Final mass (g)	5.3	4.9	4.5	3.8

The moist soil sample (28%) was also surveyed for four weeks, just like the dry soil sample. Figure 16 displays the experimental results. Table 2 illustrates that damp soil biodegrades at a faster rate than dry soil. Additionally, the product before swelling was entirely opposite to the swelled sample after approximately a week (increased by 1.05%), but the sample after swelling fell somewhat by 0.94% in the first week when comparing the two samples before and after adsorption. The material's tendency to increase in mass when in a humid environment with water present is caused by the material absorbing a certain amount of water into its structure. In contrast, the sample before swelling

in the dry soil environment as previously analyzed does not exhibit this phenomenon. Furthermore, the material before swelling did not start to enter the biodegradation process until the fourth week; in that fourth week, the material's mass dropped by roughly 0.79% from its starting value. After swelling, the sample dropped by 0.70%. Because different types of soil will have varying humidity levels and microbial populations, this indicates that the mass loss of the material increases with time and varies with the experimental setting. This is the primary cause of the material's rapid or sluggish biodegradation. For moist or even dry soil, the material after adsorption is therefore fully biodegradable, but the initial particles prior to adsorption are still biodegradable but require more time.

The findings of the study have shown that OCMCS-SAP material has better benefits than synthetic superabsorbent materials.[10,11] Despite the short survey period, it is sufficient to determine the material's gradual mass decrease. The fact that they degrade but not too quickly and that they still retain some water in their structure shows that even though the material is breaking down over time, it still guarantees the plant's access to water during its growth and development phase.

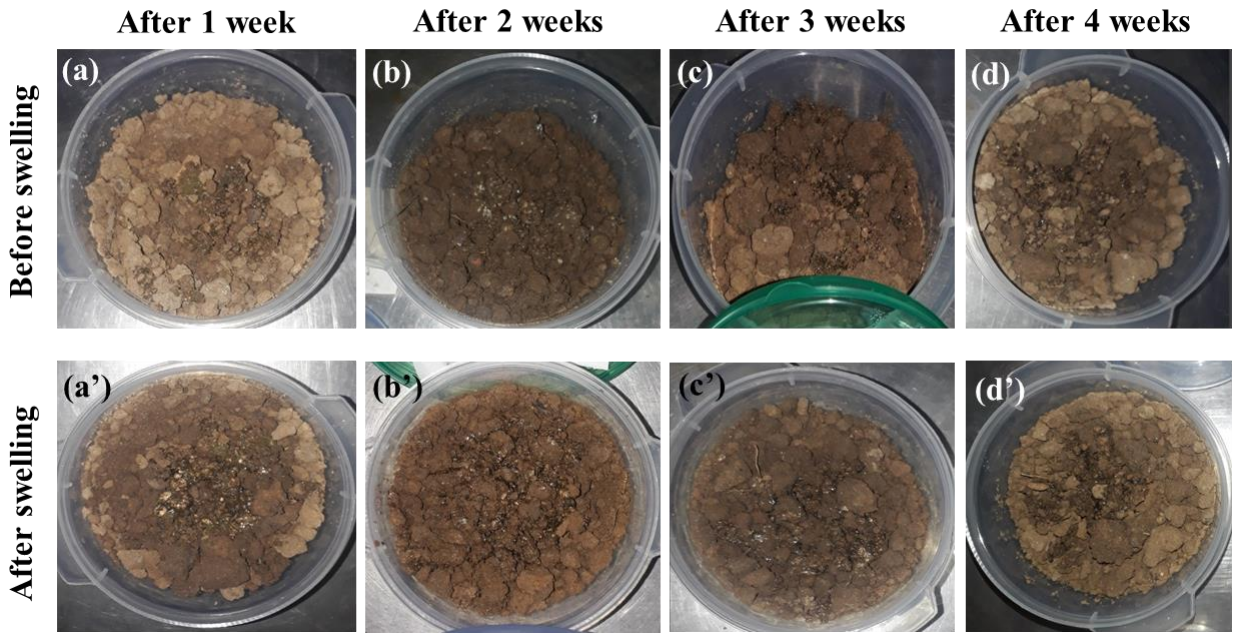

Figure 16. OCMCS-SAP samples in moist soil (humidity 28%) for biodegradation before and after swelling at different time intervals

Table 2. Experimental results of biodegradability of OCMCS-SAP on moist soil (humidity 28%) before and after adsorption at different time intervals

	After 1 week	After 2 weeks	After 3 weeks	After 4 weeks
	for OCMCS-SAP sample before adsorption			
Initial mass (g)	0.20	0.20	0.20	0.20
Final mass (g)	2.20	2.32	2.26	1.74
	for OCMCS-SAP sample after adsorption			
Initial mass (g)	5.00	5.00	5.00	5.00
Final mass (g)	5.50	5.20	4.84	3.87

3.5 Comparison of growth between two plants with and without OCMCS-SAP materials

The growth of two identical chili plants was compared over time with and without OCMCS-SAP. OCMCS-SAP particles were dissolved in water and used to water the first plant (Figure 17a), which was left unwatered for the duration of the study. During the first 10 days, the second chili plant (Figure 17b) received merely watering and was not treated with OCMCS-SAP. The observed growth of the two plants is shown in Figure 17.

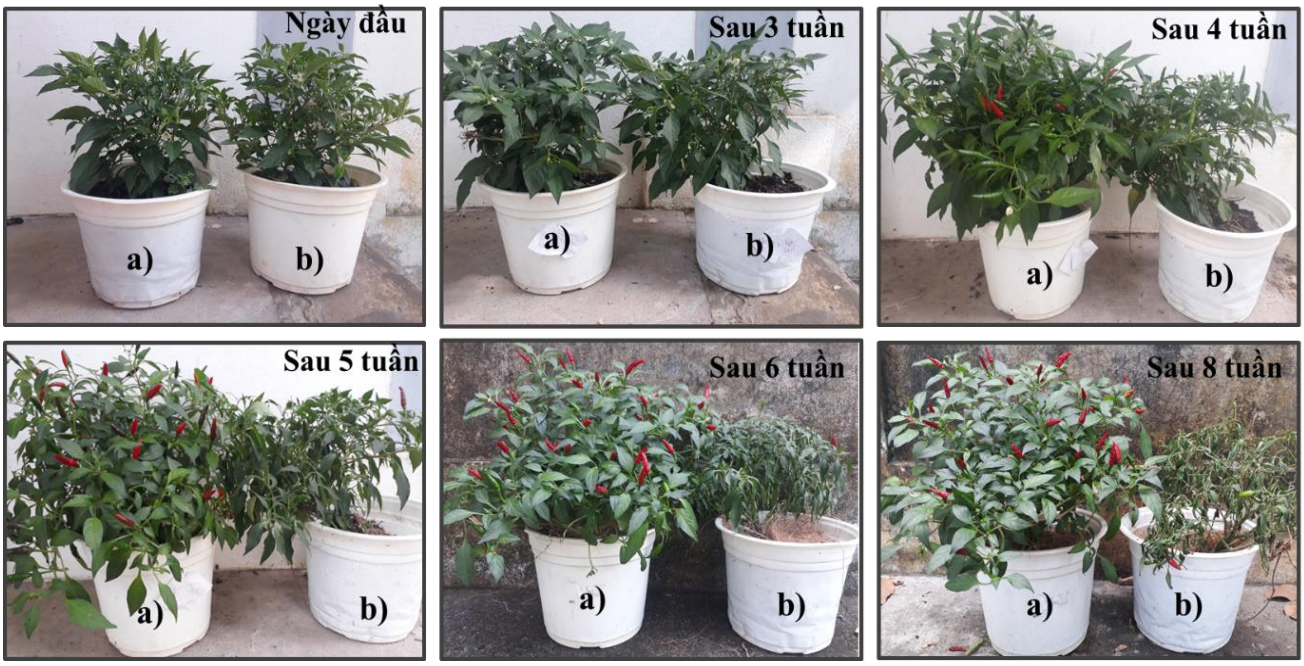

Figure 17. The distinction between two plants that (a) with and (b) without OCMCS-SAP

The initial weeks of observation showed no discernible change. In the two chili plants from the fourth week, the development was more noticeable. In comparison to the second chili plant (Figure 17b), the original chili plant (Figure 17a) grew taller, produced more fruits, and had more leaves. In contrast, the second plant (Figure 17b) did not grow taller and produced relatively few fruits. The results were more accurate by weeks five and six when the first chili plant produced a lot of fruit and continued to expand as the number of leaves increased. In contrast, the second chili plant produced nearly no fruit since it was not receiving enough water to grow and its leaves were wilting. The second plant was in danger of dying if it was not given water by the eighth week, even though the first plant was still growing and developing rapidly. The OCMCS-SAP superabsorbent material's ability to adsorb and desorb water for over eight weeks was validated in this experiment, which helped to alleviate the issue of dry soil planting areas and cut down on irrigation frequency. Additionally, study could be expanded to include the adsorption of other nutrients for plants.

4. CONCLUSIONS

The study has successfully utilized by-products in the seafood processing industry (shrimp head and body shells), which are prone to environmental pollution, to manufacture chitosan using a two-step deacetylation procedure with a high level of deacetylation. The first deacetylated chitosan had a deacetylation rate of 79.68%, whereas the second deacetylated chitosan had a high deacetylation rate of up to 91.48%. Moreover, the study successfully overcomes chitosan's poor solubility in neutral and alkaline pH environments by attaching functional groups to the main chain of chitosan, increasing chitosan's solubility in pH>6.5 environments, and then grafting the chitosan derivative with acrylic acid (AA) to create a superabsorbent polymer material from O-carboxymethyl chitosan (OCMCS-SAP). When OCMCS-SAP material was synthesized from O-carboxymethyl and acrylic acid in the presence of the cross-linking agent glutaraldehyde, it attained a maximum adsorption capacity of 658.16 g/g after 15 days of immersion in water. Simultaneously, the optimal parameters for synthesizing materials with optimal adsorption capability were 2% potassium persufate

concentration, an O-CMCS:AA ratio of 1:8, and 2% glutaraldehyde concentration.

The capacity to biodegrade (as shown by four weeks of testing) and retain water to supply the plant during its growth is a key benefit of the superabsorbent material made from O-carboxymethyl chitosan. Additionally, the study was successful in analyzing the formation and growth of two identical chili plants. Because the plants grew taller and produced more fruit, the results demonstrated that the chili plants utilizing OCMCS-SAP had much higher growth and development than those not using OCMCS-SAP. After eight weeks of testing, the unwatered plants showed wilting leaves and extremely low development. Based on all of the experimental findings, the OCMCS-SAP material has been successfully synthesized and has the potential to be applied to improve arid lands.

REFERENCES

1. N. V. Khoi. Perfecting the technology of producing superabsorbent polymer materials and applying them to retain moisture and improve soil, State level project, 2008, Ha Noi.

2. N. Nhan. God of water for plants, Science and Life Newspaper, 2006, 103.

3. H. M. G. Marzouk & Chemistry Department, Faculty of Science, Minufiya University, Minufiya (Egypt) Gamma radiation synthesis of super absorbent hydrogels for different applications, 2015.

4. A. Narayanan, R. Kartik, E. Sangeetha, R. Dhamodharan. Super water absorbing polymeric gel from chitosan, citric acid and urea: Synthesis and mechanism of water absorption, Carbohydrate polymers, 2018, 191, 152-160.

5. N. Neamjan, R. Wiwattananukul, K. Hiangrat, K. Matkaran, Y. Naiam, M. Sakulsombat, K. Sriroth. Preparation of Superabsorbent Polymer from Sugarcane Bagasse via Extrusion Process, Sugar Tech, 2019, 21(2), 296-300.

6. B. A. Yassine, M. Bezbiz, L. Belachemi, C. Moreau, C. Garnier, C. Jonchere, H. B. Youcef, B. Cathala, H. Kaddami. Preparation of superabsorbent composite(s) based on dialdehyde cellulose extracted from banana fiber waste, Carbohydrate Polymers, 2024, 343, 122504

7. J. Zhang, S. Bai, J. Lyu, X. Guan. Synthesis of a spherical starch-based superabsorbent polymer and its influence on the microstructure of hardened cement paste, Composites Part B: Engineering, 2025, 297, 112310

8. X. Guan, J. Zhang, S. Zhao, Design. Synthesis and characterization of a starch-based superabsorbent polymer and its impact on autogenous shrinkage of cement paste, Construction and Building Materials, 2024, 415, 134986

9. M. Kurniasih, P. Purwati, D. Hermawan, M. Zaki. Optimum conditions for the synthesis of high solubility carboxymethyl chitosan, Malaysian Journal of Fundamental Applied Sciences, 2014, 10(4).

10. E. M. Ahmed, M. A.H. Zahran, F. S. Aggor, S. A. A. Elhady, S. S. Nada. Synthesis and swelling characterization of carboxymethyl cellulose-g-Poly (Acrylic acid-co–Acrylamide) hydrogel and their application in agricultural field, International Journal of ChemTech Research, 2016, 9, 270-81.

11. S. Fang, G. Wang, R. Xing, X. Chen, S. Liu, Y. Qin, K. Li, X. Wang, R. Li, P. Li. Synthesis of superabsorbent polymers based on chitosan derivative graft acrylic acid-co-acrylamide and its property testing, International journal of biological macromolecules, 2019, 132, 575-584.